Radiation Measurements 142 (2021) 106546

Contents lists available at ScienceDirect

Radiation Measurements

journal homepage: http://www.elsevier.com/locate/radmeas

Radiation and temperature effect of fiber Bragg grating sensor under Co-60 irradiation

Huangfeng Ye [a], Changran Geng [a,b,c,*], Xiaobin Tang [a,b,c], Feng Tian [a], Renyao Wu [a], Pinyuan Xu [a]

[a] Department of Nuclear Science and Technology, Nanjing University of Aeronautics and Astronautics, Nanjing, 210016, China
[b] Joint International Research Laboratory on Advanced Particle Therapy, Nanjing University of Aeronautics and Astronautics, Nanjing, 210016, China
[c] Key Laboratory of Nuclear Technology Application and Radiation Protection in Astronautics, Ministry of Industry and Information Technology, Nanjing, 210016, China

ARTICLE INFO

Keywords:
Fiber Bragg gratings
Gamma rays
Radiation effects
Radiation dosimetry

ABSTRACT

This work aims to develop and characterize a mathematical algorithm for the temperature compensation of the fiber Bragg grating dosimeter and study of the effect of cumulative radiation dose on the Bragg wavelength shift (BWS). Studies on the BWS and the influence on the thermo-optic response coefficient of FBGs caused by the Co-60 gamma irradiation are performed. The BWS shows a linear dependence on temperature, and the inherent thermo-optic coefficients of the FBGs range from 10.1 to 24.0 pm/°C. The thermo-optic coefficient of FBGs is measured immediately after every 2-h irradiation. It turns out that the thermo-optic coefficient is not affected by the cumulative radiation dose and the fluctuation caused by radiation is under 2.2%. The BWS caused by 6.75 kGy gamma rays in 15 h shows a linear increase after correcting the interference of temperature. The radiation-induced coefficient is 5.18 pm/kGy and the lowest cumulative dose detection limit can be achieved at 116 Gy, which is assessed in the specific situation. The study of wavelength recovery after 3.375 kGy irradiation shows that the BWS can be recovered by around 7 pm from the 15 pm redshift, which indicates that the damage caused by the 3.5-h irradiation can be partly self-healed. This study shows the application feasibility of FBG as an online and remote radiation dosimeter.

1. Introduction

The measurement of radiation dose is needed in the field of nuclear applications such as homeland security, nuclear waste repository, and radiotherapy, as well as in other experimental or technological radiation exposure environments. Optical fiber sensors have attracted great interest for the demand of remote, online and distributed measurement of radiation fields. According to different operational principles, optical fiber sensors can be roughly classified as luminescence dosimeters, the fiber Bragg grating (FBG) sensors, distributed optical fiber sensors based on light scattering phenomena, and fiber Fabry-Perot sensors, etc. (Di Francesca et al., 2019; Faustov et al., 2015; O'Keeffe et al., 2008; Shaw et al., 2019; Zhang et al., 2018).

One of these technologies, FBG, is immune to electromagnetic interference, convenient to wavelength division multiplexing, inexpensive, flexible, thin and lightweight. Thus, FBG, including its applications in high dose radiation environments, has been widely researched (Morana et al., 2017). When FBGs were applied to monitor temperature in a high-radiation environment (such as nuclear power plant reactors), researchers found that the long-term effects of high-energy rays on FBGs caused Bragg wavelength shift (BWS), which results in considerable errors in the temperature measurement (Gusarov et al., 1999). Therefore, researchers attempted to mitigate radiation interference by using various hardening techniques for temperature monitoring (Kuhnhenn et al., 2017; Zaghloul et al., 2018). A study on the influence of different dopant and fiber pretreatment on the BWS under irradiation was conducted by Gusarov et al. (Gusarov and Hoeffgen, 2013). The BWS of gratings written on pure silica fiber or fluorine-doped fiber under radiation was less than ordinary FBG (Morana et al., 2015; Remy et al., 2016). In addition, the BWS of germanium-doped or boron-germanium co-doped FBGs under radiation was larger than that of normal ones.

With the development of new grating fabrication techniques, different grating types were studied and compared for harsh environment sensing (Blanchet et al., 2018). On the basis of the formation mechanism, FBG categories were classified into Type I, Type II, Type IIA, regenerated gratings, and femtosecond infrared laser induced gratings

* Corresponding author. Department of Nuclear Science and Technology, Nanjing University of Aeronautics and Astronautics, Nanjing, 210016, China.
E-mail address: gengchr@nuaa.edu.cn (C. Geng).

https://doi.org/10.1016/j.radmeas.2021.106546
Received 29 October 2020; Received in revised form 26 January 2021; Accepted 15 February 2021
Available online 18 February 2021
1350-4487/

(Birri et al., 2019; Mihailov, 2012; Morana et al., 2018; Tu et al., 2017). However, the BWS phenomenon of FBGs under radiation could be used for radiation sensing (Krebber et al., 2006; Broadway et al., 2019). Therefore, methods were also investigated to enhance radiation sensitivity. Hydrogen-loading was applied before writing to improve the radiation sensitivity of the FBGs (Slattery et al., 2005). Forming resonant cavities or using long-period gratings is an advanced method to enhance radiation sensitivity used in recent years (Avino et al, 2013, 2015; Esposito et al., 2017; Sporea et al., 2016). Thus, FBG is a promising candidate for radiation dosimeter. FBG is sensitive to multiple parameters, which leads to a cross-sensitivity issue (Yang et al., 2013). Temperature cross-sensitivity is a crucial problem that needs to be solved before the practical application of FBGs to radiation field dose measurement.

In this study, we investigated the effects of radiation and temperature on Type I FBGs written on optical fiber. To improve the sensitivity of FBGs in measuring doses in a radiation field, the dependence of temperature on bare FBGs was measured. The relationship between thermo-optical response coefficient and dose was discussed. Then a method of temperature effect correction was applied to the study of dose dependence of BWS. Lastly, the relaxation of BWS was studied after irradiation.

2. Materials and methods

2.1. FBG manufacturing and equipment

Nine FBGs of the same type were written on SMF-28 (Corning, Shanghai/China) whose core/cladding diameter is 9/125 μm, respectively; FBGs were produced by the Hope-Excellence Information Technology Co., Ltd (HE) in Beijing, China. The fiber was pre-hydrogenated for 300 h at 110 bars at room temperature. Type I FBGs were written on hydrogen-loaded fiber using excimer laser and phase mask and recoated with acrylate after writing. In the process of recoating, FBGs were recoated with acrylate using a mini-coater, suffered different number of UV curing cycle and a post-recoating thermal treatment (Blanchet et al., 2018). The length of each FBG was 5 mm and the Bragg wavelengths of the fibers ranged from 1530 nm to 1565 nm. FBGs were taped tightly on a 10×10 cm^2 PMMA pad with polyimide tape. As a temperature sensor, Pt100 thermal resistance (Heraeus, Hanau/Germany) was also fixed close to the FBGs on the PMMA pad. Through a resistance current transmitter, Pt100 could realize remote temperature measurement with accuracy guarantee of 0.1 °C.

To resolve the reflected Bragg wavelength in the FBGs, the FBG demodulator used in this study was SuperHawk6000 (Beijing Hope-Excellence, Beijing/China) which was based on the principle of tunable fiber Fabry-Perot (TFFP) filter. It is equipped with a wide-spectrum light source to emit laser light along the fiber, and demodulates the spectrum reflected from the FBG. The BWS was obtained

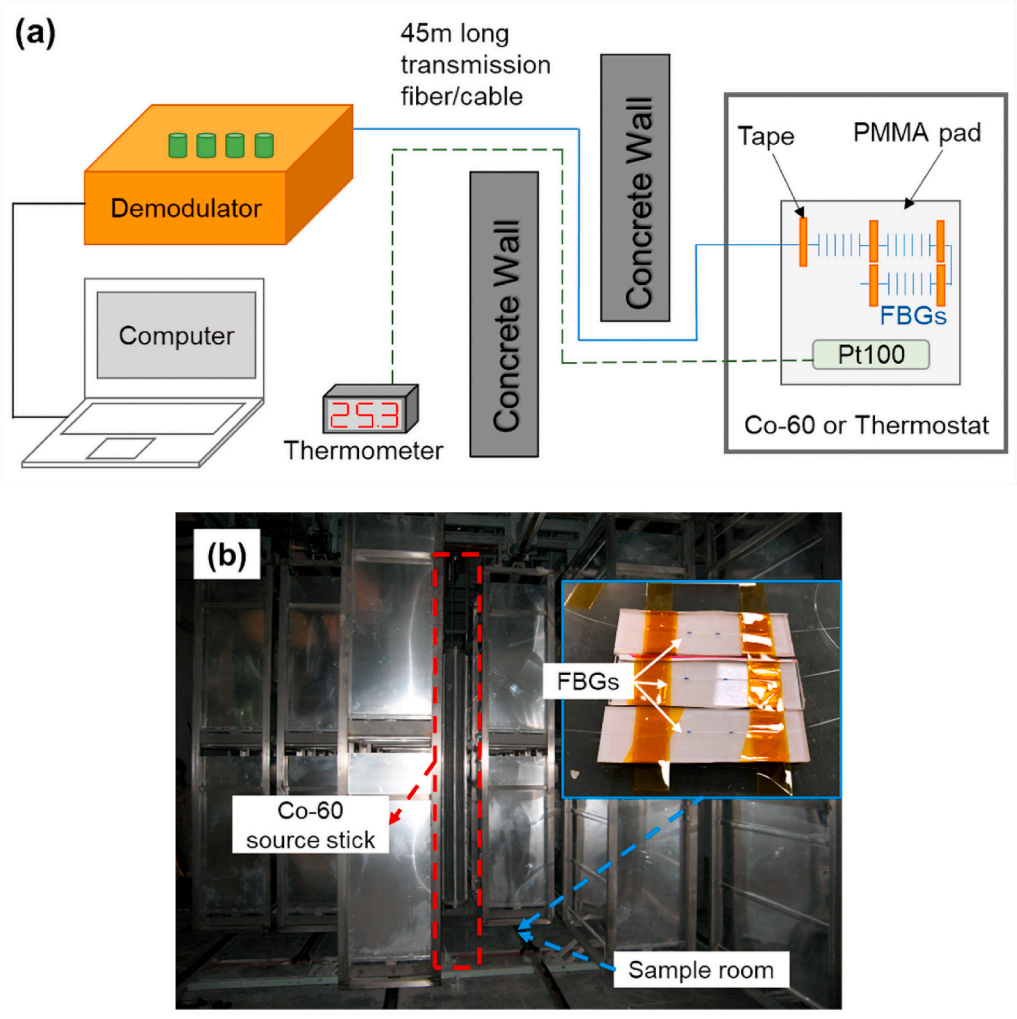

Fig. 1. Schematic of (a) the experiment setup and (b) actual irradiation placement.

by calculating the difference of the Bragg wavelength data with and without the effect of external sources. SuperHawk6000 can achieve a high wavelength resolution of approximately 0.7 pm in the working wavelength range of 1528 nm–1568 nm. Its wavelength accuracy is 1 pm and its scan frequency is tunable from 1 Hz to 100 Hz.

2.2. Test condition and experimental procedure

The FBGs were irradiated using an industrial Co-60 gamma source at a dose rate of 0.45 kGy/h. The silver dichromate dosimeter was used in calibrating the dose rate and the accumulative doses during the experiment.

As shown in Fig. 1(a), when analyzing the temperature dependence of the Bragg wavelength, FBGs were located in a temperature-controlled thermostat with no radiation rays and the central wavelength of the Bragg peak in the back reflection was recorded by the demodulator. FBGs wrapped with aerogel felt were under Co-60 gamma ray when the effect of gamma exposure on the reflectance wavelength was under discussion. Real-time signal was transmitted through a 45-m-long fiber/cable. With a radioactive source dipped into a water pool after irradiation, a relaxation experiment was performed, and the reflection wavelength of the FBG was recorded as a comparison to the initial value and determined as a function of the relaxation time. The photograph of the experiment setup is shown in Fig. 1(b). The red dotted frame in the image is the position of the Co-60 source stick and the sample room for the irradiation experiment was set near the bottom of the source shelf. The FBGs were kept unstrained during the entire experiment to avoid complications related with strain sensitivity.

3. Results and discussion

3.1. Temperature dependence of the Bragg wavelength in FBGs

The Bragg wavelength equation is given by,

$$\lambda_B = 2n_{eff}\Lambda \quad (1)$$

where λ_B is the peak wavelength at the Bragg back reflection, n_{eff} is the effective refractive index and Λ is the grating period (Kinet et al., 2014).

In the case of stress-free FBG, the reflection Bragg wavelength λ_B shifts proportionally with the temperature. The BWS as a function of temperature can be calculated by,

$$\Delta\lambda_B = K_T\Delta T \quad (2)$$

where K_T is the thermo-optical response coefficient, which can be obtained through curve fitting. The values of $\Delta\lambda_B$ and ΔT were acquired from measurement.

In this section, the dependence of temperature on the bare FBG was first studied separately, and the relationship between the Bragg wavelength of the FBG and the temperature change was obtained.

The BWSs with temperature for each FBG are shown in Fig. 2, in which the data have been normalized to the Bragg wavelength at 25 °C. The solid line is the fitting curve of BWS versus temperature. The BWS shows a linear dependence with the temperature at a wide range (from 0 °C to 60 °C) as illustrated. The BWSs versus temperature for the nine FBGs are plotted in Fig. 2(b).

In accordance with Formula (2), the thermo-optical response coefficient of $\lambda_B$for each FBG was fitted by linear regression using the least squares method. Consistent with previous results, the R-square of the linearity of the fitting line is greater than 0.99. The thermo-optical coefficients of the FBGs in the experiment are listed in Table 1. The inherent temperature sensitivity of FBGs varied from 10.1 pm/°C to 24.0 pm/°C even if the same fiber type and the same writing process were used. This is because one step in the manufacturing procedure is that the Type I FBG requires the coating of a specific fiber section to be stripped before being written. The FBG was finally recoated for durability and the instability of manual recoating for several times may have caused the temperature sensitivity difference.

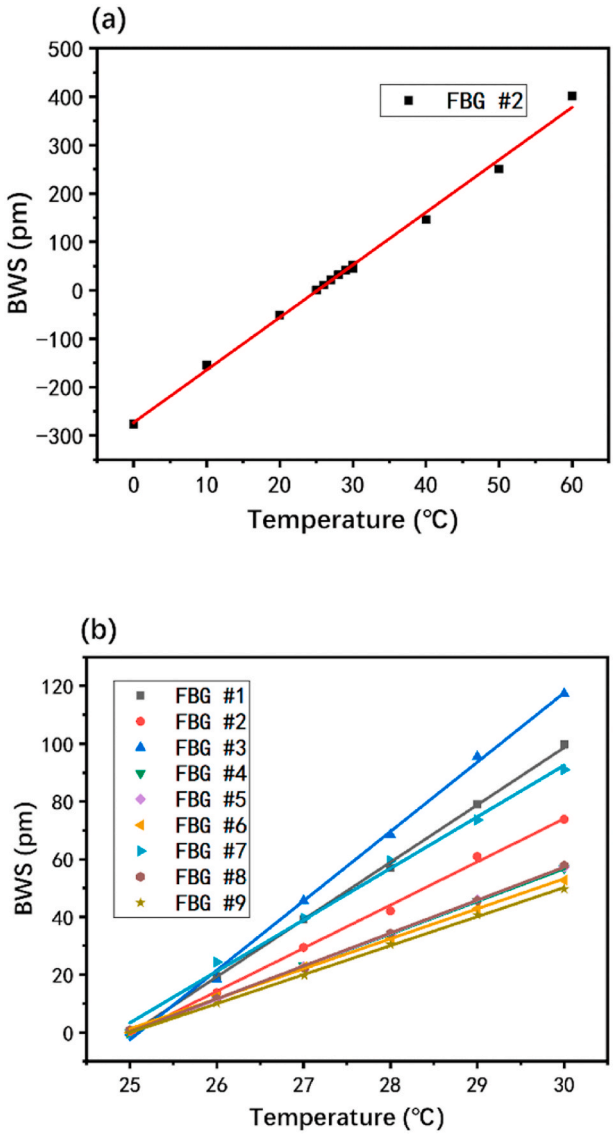

Fig. 2. (a) Bragg wavelength shift of the FBG under the temperature from 0 °C to 60 °C; (b) Bragg wavelength shifts of nine FBGs under the temperature from 25 °C to 30 °C.

Table 1
Thermo-optical response coefficient of each FBG used in this work.

FBG label	K_T(pm/°C)	FBG label	K_T(pm/°C)	FBG label	K_T(pm/°C)
1	19.9	4	11.3	7	17.8
2	14.9	5	11.5	8	11.4
3	24.0	6	10.4	9	10.1

3.2. Radiation dose response of the thermo-optical response coefficient in FBGs

When using FBG sensor to measure radiation dose, its application in an environment where radiation and temperature coexist is inevitable. In consideration of the lessons from the study of the joint effect of temperature and strain, the contribution of radiation and temperature to the Bragg wavelength are assumed to be two independent parts (Kinet et al., 2014). The total BWS of FBG under radiation detection application

can be proposed as

$$\Delta\lambda_B(D,T) = \Delta\lambda_B(D) + \Delta\lambda_B(T) = \Delta\lambda_B(D) + K_T\Delta T \quad (3)$$

To compensate for the temperature effect, the radiation-induced BWS $\Delta\lambda_B(D)$ was obtained by subtracting the temperature-induced BWS, which is the product of thermo-optical response coefficient $K_T$and temperature change ΔT, from the total BWS $\Delta\lambda_B(D,T)$.

Avino et al. reported a fiber-optic resonant cavity based on two FBGs or one π phase-shifted FBG to detect ionizing radiation (Avino et al, 2013, 2015). Both ionizing radiation detectors were observed remarkable variations of the fiber thermo-optic coefficient after irradiation in clinical linear accelerators. Kinet et al. confirmed that the FBG temperature sensitivity, which also means thermo-optical response coefficient, distinctly decreased after irradiation (Kinet et al., 2019). A few references have mentioned the regularity of the thermo-optic response coefficient after irradiation; therefore, the use of the thermo-optic response coefficient to characterize the accumulated radiation dose is also worth studying. If using this parameter is feasible, then the need for temperature recording throughout the process can be eliminated. However, some researchers reported a different result. Henschel et al. presented a repeated measurement of temperature sensitivity with a FBG after its irradiation up to 1 MGy resulted within limits of error similar to the sensitivity of unirradiated fiber (10.04 instead of 10.41 pm/°C) (Henschel et al., 2009). Gusarov and Hoeffgen found that the temperature sensitivity coefficients were not affected by radiation within the accuracy of measurements (smaller than ±0.2 pm/°C in all cases; ±2%) (Gusarov and Hoeffgen, 2013). Blanchet et al. also confirmed that the thermal sensitivity coefficient did no change with the irradiation within an error of 2% (obtained at 250 °C) (Blanchet et al., 2019).

In this section, the method of repeated irradiation was used to obtain $K_T$after each irradiation for verification. The FBGs underwent 2-h irradiation for three times; the measurement of thermo-optic coefficient was performed immediately after irradiation. The relationship of the thermo-optic response coefficient with the cumulative dose was analyzed in Figs. 3 and 4.

FBG #6–0, #6–1, #6–2 and #6–3 in Fig. 3 denote FBG #6 before irradiation and after one, two, and three rounds of a 2-h irradiation, respectively. Only the result of FBG #6 is presented here because the results of other FBGs are similar. The $K_T$values of FBG #5 and #6 under different conditions are presented in Fig. 4. The results show that the thermo-optic response coefficient is not affected by the cumulative radiation dose and continues to fluctuate within the error range (under

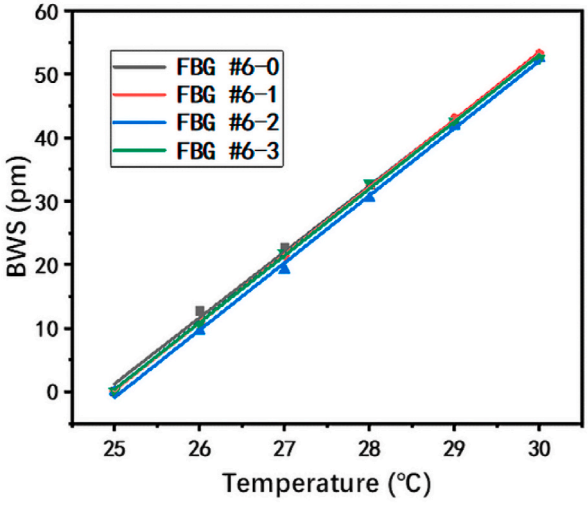

Fig. 3. Temperature dependence of BWS of same FBG with different irradiation times.

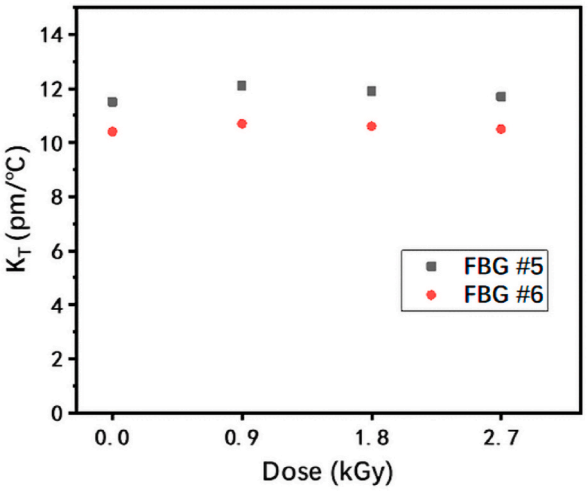

Fig. 4. Dependence of thermo-optical response coefficient with different cumulative doses.

2.2%). This result supports most of the literature results but slightly different from the experimental results of Avino and Kinet (Avino et al, 2013, 2015; Kinet et al., 2019). These differences are partly due to the different FBGs used. In general, K_T measured before irradiation is equivalent to K_T during irradiation and the effectiveness of the calculation method using Formula (3) is verified.

3.3. Radiation dose response of the Bragg wavelength in FBGs

In this section, an aerogel material was used to provide a certain degree of insulation for a 15-h irradiation experiment. Although the adiabatic treatment was performed, approximately 1 °C ambient temperature fluctuation was still observed between day and night within 15 h. These temperature values with an accuracy less than 0.1 °C were measured simultaneously during Bragg wavelength interrogation. The wavelength change under the combined inducement of temperature and radiation was recorded directly, and the separate radiation-induced wavelength change was calculated using Formula (3).

FBGs labeled 1, 2, 3 were used for research on responses to repeated radiation doses. The uncorrected and corrected shifts for investigated FBGs during the irradiation experiment is shown in Fig. 5.

In Fig. 5(a), the direct output without temperature correction is the BWS under the combined action of the two parameters, and the cross-sensitivity result makes it unfavorable for direct dosimetry application. Fig. 5(b)(c) show a continuous increase in $\Delta\lambda_B(D)$ with the radiation dose after correction (result of FBG #3 is similar to that of FBG #1, #2). Up to 6.75 kGy, any saturation of BWS is not observed for all FBGs because the accumulated dose was not high enough to saturate as observed in a previous work (Blanchet et al., 2019). Approximately, the BWS caused by 15-h gamma rays irradiation shows a certain linear relationship. Taking FBG #1 for example, the maximum wavelength shift was 35 pm and the radiation-induced coefficient is 5.18 pm/kGy. The Bragg wavelength measurement error during one laser interrogation is approximately 0.6 pm, thus the lowest cumulative dose detection limit can be achieved at 116 Gy with the set of equipment applied in this work. Broadway et al. presented a polymer fiber Bragg grating sensor and calculated a sensitivity of −26.2 pm/kGy and a resolution of 40 Gy over a total dose of 41 kGy (Broadway et al., 2019). This detection limit is probably limited by the radiation sensitivity of FBG and the performance of demodulation equipment. For high-dose radiation dosimetry such as industrial measurement application and experiment monitoring of large-scale scientific devices, this combination of FBG and demodulator is suitable. To obtain a lower detection limit in a low-dose situation

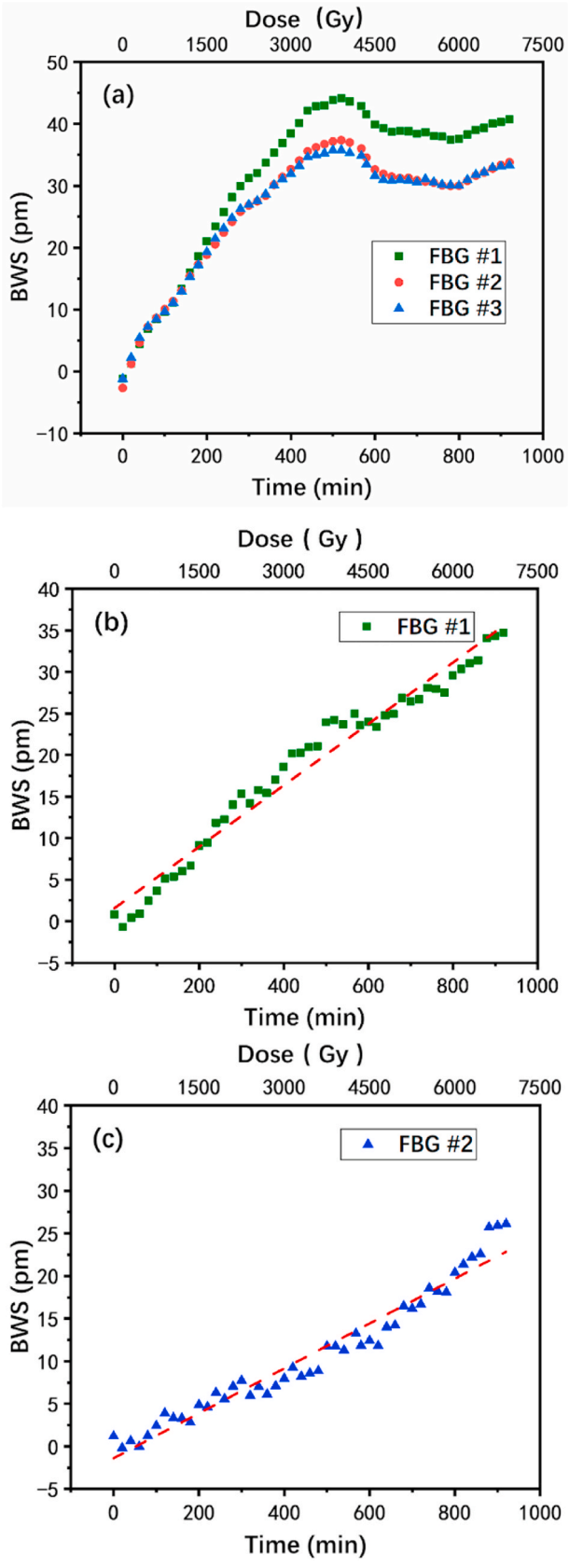

Fig. 5. (a) The BWS under irradiation without the temperature contribution correction; (b)(c) The BWS under irradiation with the temperature contribution correction.

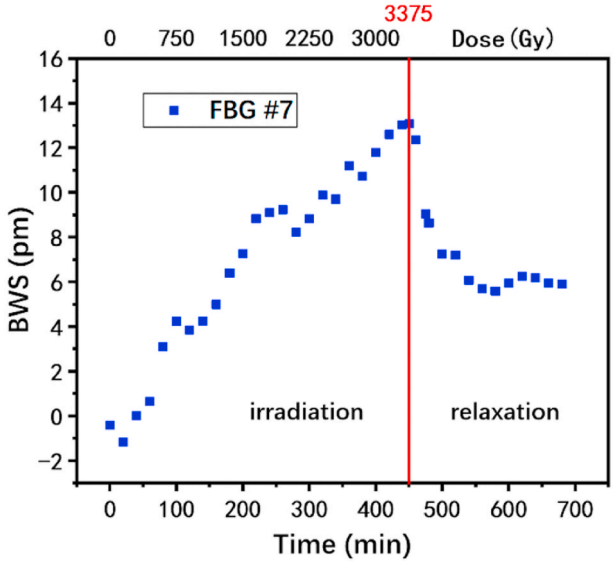

Fig. 6. Bragg wavelength shift of the FBG during irradiation (0–450 min, left part of the red line) and relaxation (450–660 min, right part of the red line). (For interpretation of the references to colour in this figure legend, the reader is referred to the Web version of this article.)

(even for radiotherapy level), follow-up research can focus on increasing special dopant content (such as germanium) in the fiber core material or an instrument with higher wavelength measurement accuracy.

The radiation response coefficients of these FBGs are kind of different even if the same fiber is written by the same manufacturer under the same conditions. This result may be related to the photosensitivity of the fiber itself (caused by locally uneven dopant, hydrogen permeation efficiency, and manual operation difference etc.).

3.4. Relaxation of BWS in FBGs

To determine the reliability of FBG for multiple use as a radiation dosimeter, research must be conducted on the recovery time of BWS after irradiation and the degree of damage to the FBG caused by radiation during detection. Another three FBGs (labeled 7, 8, 9) were used in this part of irradiation. After 7.5 h of irradiation, we lowered the source into the water tank and kept it for 3.5 h to allow the wavelength to self-recover. During the period the change of the wavelength shift after irradiation was recorded.

Fig. 6 shows the effect of relaxation for FBGs after a total irradiation dose of 3.375 kGy (accumulated 7.5 h at 0.45 kGy/h). The left part of the red line in the figure is the BWS of irradiation and the right part is the relaxation part without radiation. In the experiment, gamma rays cause a continuous redshift on fiber Bragg wavelength to 13 pm, with temperature contribution corrected. After stopping irradiation for 3.5 h, the wavelength relaxes 7 pm back and then remains stable. That is, the effect of the removal of the Co-60 gamma source and the relaxation of the shifted Bragg wavelength can partly recover. The damage of 3.375 kGy to this specific FBG is semi-permanent in 3.5 h. When FBGs are taken out to measure BWS after being irradiated as an offline dosimeter, this slight wavelength recovery phenomenon may cause inaccuracy of the actual measured value and finally brings errors in characterizing radiation dose. As a result, this kind of dosimeter can be used as an online measurement and has certain limitations if applied as an offline measurement method.

4. Conclusion

This work develops and characterizes a method for the temperature compensation of the fiber Bragg grating dosimeter and studies the effect

of cumulative radiation dose on the Bragg wavelength shift. Studies on the BWS and the influence on the thermo-optic response coefficient of FBGs caused by the Co-60 gamma irradiation are performed. The BWS shows a linear dependence on the temperature change within a wide range (from 0 °C to 60 °C). A continuous increase in $\Delta\lambda_B(D)$ with the radiation dose can be observed after the correction of temperature effect and no saturation of BWS is observed for all FBGs. Taking FBG #1 for example, the radiation response coefficient is approximately 5.18 pm/kGy and the device used in this work can achieve the lowest 116 Gy cumulative dose detection limit. The application feasibility of the FBG radiation dosimeter that uses the thermo-optic response coefficient to compensate the temperature effect is verified. The relaxation phenomenon makes the dosimeter more suitable for online measurement rather than offline measurement. Using the wavelength division multiplexing characteristics of FBGs in optical fiber networks, and cooperating with ultra-low loss optical fiber communication to transmit optical signals, it is possible to achieve remote online monitoring of dose distribution in the radiation field.

Declaration of competing interest

The authors declare that they have no known competing financial interests or personal relationships that could have appeared to influence the work reported in this paper.

Acknowledgements

This work was supported by the National Natural Science Foundation of China [Grant No. 11805100, Grant No. 12075120], the Natural Science Foundation of Jiangsu Province [Grant No. BK20180415] and China Postdoctoral Science Foundation [Grant No. 2019M651829].

References

Avino, S., D'Avino, V., Giorgini, A., Pacelli, R., Liuzzi, R., Cella, L., De Natale, P., Gagliardi, G., 2015. Ionizing radiation detectors based on ge-doped optical fibers inserted in resonant cavities. Sensors 15, 4242–4252. https://doi.org/10.3390/s150204242.

Avino, S., D'Avino, V., Giorgini, A., Pacelli, R., Liuzzi, R., Cella, L., De Natale, P., Gagliardi, G., 2013. Detecting ionizing radiation with optical fibers down to biomedical doses. Appl. Phys. Lett. 103, 184102. https://doi.org/10.1063/1.4826934.

Birri, A., Wilson, B.A., Blue, T.E., 2019. Deduced refractive index profile changes of type i and type II gratings when subjected to ionizing radiation. IEEE Sensor. J. 19, 5000–5006. https://doi.org/10.1109/JSEN.2019.2904013.

Blanchet, T., Morana, A., Laffont, G., Cotillard, R., Marin, E., Boukenter, A., Ouerdane, Y., Girard, S., 2018. Radiation effects on type i fiber bragg gratings: influence of recoating and irradiation conditions. J. Lightwave Technol. 36, 998–1004. https://doi.org/10.1109/JLT.2018.2791640.

Blanchet, T., Nehr, S., Desmarchelier, R., Morana, A., Gusarov, A., Boukenter, A., Ouerdane, Y., Marin, E., Girard, S., Laffont, G., 2019. High temperature and γ-ray radiation effects on regenerated fiber bragg grating. Opt. InfoBase Conf. Pap. Part F166, 4763–4769. https://doi.org/10.1364/SENSORS.2019.STh4A.5.

Broadway, C., Kinet, D., Theodosiou, A., Kalli, K., Gusarov, A., Caucheteur, C., Mégret, P., 2019. CYTOP fibre bragg grating sensors for harsh radiation environments. Sensors 19, 2853. https://doi.org/10.3390/s19132853.

Di Francesca, D., Vecchi, G.L., Girard, S., Morana, A., Reghioua, I., Alessi, A., Hoehr, C., Robin, T., Kadi, Y., Brugger, M., 2019. Qualification and calibration of single-mode phosphosilicate optical fiber for dosimetry at CERN. J. Lightwave Technol. 37, 4643–4649. https://doi.org/10.1109/JLT.2019.2915510.

Esposito, F., Ranjan, R., Stăncălie, A., Sporea, D., Neguţ, D., Becherescu, N., Campopiano, S., Iadicicco, A., 2017. Real-time analysis of arc-induced Long Period Gratings under gamma irradiation. Sci. Rep. 7, 43389. https://doi.org/10.1038/srep43389.

Faustov, A.V., Gusarov, A.V., Mégret, P., Wuilpart, M., Zhukov, A.V., Novikov, S.G., Svetukhin, V.V., Fotiadi, A.A., 2015. The use of optical frequency-domain reflectometry in remote distributed measurements of the γ-radiation dose. Tech. Phys. Lett. 41, 414–417. https://doi.org/10.1134/S1063785015050053.

Gusarov, A., Hoeffgen, S.K., 2013. Radiation effects on fiber gratings. IEEE Trans. Nucl. Sci. 60, 2037–2053. https://doi.org/10.1109/TNS.2013.2252366.

Gusarov, A.I., Starodubov, D.S., Berghmans, F., Deparis, O., Defosse, Y., Fernandez, A.F., Decreton, M.C., Megret, P., Blondel, M., 1999. Design of a radiation-hard optical fiber Bragg grating temperature sensor. In: Photonics for Space and Radiation Environments. International Society for Optics and Photonics, p. 43. https://doi.org/10.1117/12.373284.

Henschel, H., Hoeffgen, S.K., Kuhnhenn, J., Weinand, U., 2009. Influence of manufacturing parameters and temperature on the radiation sensitivity of fiber Bragg gratings. In: Proceedings of the European Conference on Radiation and its Effects on Components and Systems. RADECS. IEEE, pp. 382–387. https://doi.org/10.1109/RADECS.2009.5994682.

Kinet, D., Broadway, C., Gusarov, A., Mégret, P., Caucheteur, C., 2019. Fibre Bragg gratings wavelength evolution and thermal sensitivity under gamma irradiation. In: Seventh European Workshop on Optical Fibre Sensors. International Society for Optics and Photonics, p. 55. https://doi.org/10.1117/12.2539967.

Kinet, D., Mégret, P., Goossen, K.W., Qiu, L., Heider, D., Caucheteur, C., 2014. Fiber Bragg grating sensors toward structural health monitoring in composite materials: challenges and solutions. Sensors 14, 7394–7419. https://doi.org/10.3390/s140407394.

Krebber, K., Henschel, H., Weinand, U., 2006. Fibre Bragg gratings as high dose radiation sensors? Meas. Sci. Technol. 17, 1095–1102. https://doi.org/10.1088/0957-0233/17/5/S26.

Kuhnhenn, J., Weinand, U., Morana, A., Girard, S., Marin, E., Périsse, J., Genot, J.S., Grelin, J., Hutter, L., Mélin, G., Lablonde, L., Robin, T., Cadier, B., MacÉ, J.R., Boukenter, A., Ouerdane, Y., 2017. Gamma radiation tests of radiation-hardened fiber Bragg grating based sensors for radiation environments. Proc. Eur. Conf. Radiat. its Eff. Components Syst. RADECS 2016-Septe 1–4. https://doi.org/10.1109/RADECS.2016.8093133.

Mihailov, S.J., 2012. Fiber bragg grating sensors for harsh environments. Sensors 12, 1898–1918. https://doi.org/10.3390/s120201898.

Morana, A., Girard, S., Marin, E., Lancry, M., Grelin, J., Marcandella, C., Paillet, P., Boukenter, A., Ouerdane, Y., 2018. Dependence of the voids-fiber bragg grating radiation response on temperature, dose, and dose rate. IEEE Trans. Nucl. Sci. 65, 1619–1623. https://doi.org/10.1109/TNS.2017.2778882.

Morana, A., Girard, S., Marin, E., Marcandella, C., Rizzolo, S., Périsse, J., Macé, J.R., Taouri, A., Boukenter, A., Cannas, M., Ouerdane, Y., 2015. Radiation vulnerability of fiber bragg gratings in harsh environments. J. Lightwave Technol. 33, 2646–2651. https://doi.org/10.1109/JLT.2014.2364526.

Morana, A., Girard, S., Marin, E., Périsse, J., Genot, J.S., Kuhnhenn, J., Grelin, J., Hutter, L., Mélin, G., Lablonde, L., Robin, T., Cadier, B., Macé, J.R., Boukenter, A., Ouerdane, Y., 2017. Radiation-Hardened fiber bragg grating based sensors for harsh environments. IEEE Trans. Nucl. Sci. 64, 68–73. https://doi.org/10.1109/TNS.2016.2621165.

O'Keeffe, S., Fitzpatrick, C., Lewis, E., Al-Shamma'A, A.I., 2008. A review of optical fibre radiation dosimeters. Sens. Rev. 28, 136–142. https://doi.org/10.1108/02602280810856705.

Remy, L., Cheymol, G., Gusarov, A., Morana, A., Marin, E., Girard, S., 2016. Compaction in optical fibres and fibre bragg gratings under nuclear reactor high neutron and gamma fluence. IEEE Trans. Nucl. Sci. 63, 2317–2322. https://doi.org/10.1109/TNS.2016.2570948.

Shaw, R.E., Kalnins, C.A.G., Spooner, N.A., Whittaker, C., Grimm, S., Schuster, K., Ottaway, D., Moffatt, J.E., Tsiminis, G., Ebendorff-Heidepriem, H., 2019. Luminescence effects in reactive powder sintered silica glasses for radiation sensing. J. Am. Ceram. Soc. 102, 222–238. https://doi.org/10.1111/jace.15918.

Slattery, S.A., Nikogosyan, D.N., Brambilla, G., 2005. Fiber Bragg grating inscription by high-intensity femtosecond UV laser light: comparison with other existing methods of fabrication: erratum. J. Opt. Soc. Am. B 22, 1143. https://doi.org/10.1364/josab.22.001143.

Sporea, D., Stăncalie, A., Neguţ, D., Delepine-Lesoille, S., Lablonde, L., 2016. Long period grating response to gamma radiation. In: Micro-Structured and Specialty Optical Fibres IV. International Society for Optics and Photonics, p. 98861. https://doi.org/10.1117/12.2230233.

Tu, Y., Ye, L., Zhou, S.P., Tu, S.T., 2017. An improved metal-packaged strain sensor based on a regenerated fiber bragg grating in hydrogen-loaded boron–germanium co-doped photosensitive fiber for high-temperature applications. Sensors 17, 431. https://doi.org/10.3390/s17030431.

Yang, G., Lin, S., Jin, J., Song, N., 2013. Effect of gamma radiation on the reflectance spectrum of fiber Bragg gratings. Optik 124, 2246–2250. https://doi.org/10.1016/j.ijleo.2012.06.083.

Zaghloul, M.A.S., Wang, M., Huang, S., Hnatovsky, C., Grobnic, D., Mihailov, S., Li, M.-J., Carpenter, D., Hu, L.-W., Daw, J., Laffont, G., Nehr, S., Chen, K.P., 2018. Radiation resistant fiber Bragg grating in random air-line fibers for sensing applications in nuclear reactor cores. Optic Express 26, 11775. https://doi.org/10.1364/oe.26.011775.

Zhang, X., Tang, X., Shu, D., Gong, C., Geng, C., Ai, Y., Yu, H., Shao, W., 2018. Theoretical calculation and measurement accuracy of Cerenkov optic-fiber dosimeter under electron and photon radiation therapies. Radiat. Meas. 110, 1–6. https://doi.org/10.1016/j.radmeas.2018.01.001.